

## Purdue University Purdue e-Pubs

---

Department of Electrical and Computer  
Engineering Faculty Publications

Department of Electrical and Computer  
Engineering

---

2006

# Ballisticity of nanotube field-effect transistors: Role of phonon energy and gate bias

Siyuranga O. Koswatta  
*Purdue University*, [koswatta@purdue.edu](mailto:koswatta@purdue.edu)

Sayed Hasan  
*Purdue University*

Mark S. Lundstrom  
*Purdue University*, [lundstro@purdue.edu](mailto:lundstro@purdue.edu)

Follow this and additional works at: <https://docs.lib.purdue.edu/ecepubs>

 Part of the [Electrical and Computer Engineering Commons](#)

---

Koswatta, Siyuranga O.; Hasan, Sayed; and Lundstrom, Mark S., "Ballisticity of nanotube field-effect transistors: Role of phonon energy and gate bias" (2006). *Department of Electrical and Computer Engineering Faculty Publications*. Paper 150.  
<http://dx.doi.org/10.1063/1.2218322>

This document has been made available through Purdue e-Pubs, a service of the Purdue University Libraries. Please contact [epubs@purdue.edu](mailto:epubs@purdue.edu) for additional information.

# Ballisticity of nanotube field-effect transistors: Role of phonon energy and gate bias

Siyuranga O. Koswatta, Sayed Hasan, and Mark S. Lundstrom

*School of Electrical and Computer Engineering, Purdue University, West Lafayette, Indiana 47907-1285*

M. P. Anantram

*Center for Nanotechnology, NASA Ames Research Center, 229-1, Moffett Field, California 94035*

Dmitri E. Nikonov<sup>a)</sup>

*Technology and Manufacturing Group, Intel Corp., SC1-05, Santa Clara, California 95052*

(Received 30 November 2005; accepted 26 May 2006; published online 14 July 2006)

We investigate the role of electron-phonon scattering and gate bias in degrading the drive current of nanotube field-effect transistors (FETs). Optical phonon scattering significantly decreases the drive current only when gate voltage is higher than a well-defined threshold. For comparable electron-phonon coupling, a lower phonon energy leads to a larger degradation of drive current. Thus in semiconductor nanowire FETs, the drive current will be more sensitive than in carbon nanotube FETs because of the smaller phonon energies in semiconductors. Acoustic phonons and other elastic scattering mechanisms are most detrimental to nanotube FETs irrespective of biasing conditions. © 2006 American Institute of Physics. [DOI: 10.1063/1.2218322]

Interconnects and field-effect transistors (FETs) based on, respectively, metallic and semiconducting carbon nanotubes (CNTs) have received considerable attention over the last five years because their performance metrics make them promising electronic devices. Experiments have established that transport in metallic carbon nanotube wires is close to the ballistic limit at biases smaller than approximately 100 meV.<sup>1,2</sup> At larger biases, the current carrying capacity of metallic nanotubes is far from ballistic due to zone boundary and optical phonon scattering.<sup>3-6</sup> For nanotube FETs, experiments have demonstrated near-ballistic transport<sup>7</sup> and on-current performance that exceeds that of silicon transistors.<sup>7,8</sup> Our objective in this letter is to provide insight into how various electron-phonon scattering mechanisms and the applied gate bias affect the on current of a carbon nanotube FET. Recent work showed that elastic scattering can strongly degrade the on current but strong optical phonon scattering may have little effect.<sup>9</sup> This work extends prior work<sup>9-14</sup> by examining the phonon modes most likely to couple to electrons, by using a fully quantum mechanical approach, and by exploring the gate bias dependence of electron-phonon scattering in a CNT metal-oxide-semiconductor field-effect transistor (MOSFET). We show that the radial breathing mode may play an important role in some experiments, and the gate bias dependence displays a clear threshold effect. We confirm that the on current of a CNT MOSFET is much more sensitive to elastic scattering than to inelastic scattering.

The current-voltage characteristics are calculated using the nonequilibrium Green's function (NEGF) approach,<sup>15</sup> where the charge density is calculated using the efficient algorithm of Ref. 16. The NEGF transport equations are solved in mode space using the  $\pi$  orbital tight binding Hamiltonian, self-consistently with Poisson's equation.<sup>17</sup> Electron-phonon scattering is treated within the mode space approach in a manner similar to that in Refs. 9 and 16, but we carefully consider both the longitudinal ( $L$ ) and transverse ( $T$ ) optical

phonon (OP) and acoustic phonon (AP) branches, and the radial breathing modes (RBMs).<sup>18</sup> In this letter we disregard the real part of the self-energy and focus on the imaginary part which describes scattering.

The CNT MOSFET structure employed in this study is a (13,0) zigzag CNT with band gap  $E_G=0.8$  eV and channel length  $L_G=20$  nm, and high- $k$  HfO<sub>2</sub> cylindrical gate with  $k=16$  and thickness  $t_{ox}=2$  nm. Source and drain doping is 1.5 dopant atoms/nm [for comparison, (13,0) CNT has 122 carbon atoms/nm]. The lowest electronic subbands in the (13,0) nanotube correspond to two degenerate valleys with azimuthal quantum numbers  $m=9$  and  $m=17$ . Therefore the phonons with azimuthal quantum numbers of  $m=0$  cause intravalley transitions, and phonons with  $m=8$  cause the intervalley transitions (also known as zone-boundary scattering). For moderate biases, electrons are concentrated close to the band minima, and we can consider phonons with  $q \approx 0$  (long wavelength). The optical and RBM phonon modes considered in this study are calculated according to Ref. 18, and the corresponding electron-phonon coupling (EPC) constants are summarized in Table I. The electron-phonon coupling strengths for these modes in an  $(n,0)$  zigzag CNT are determined by

TABLE I. Phonon modes and corresponding coupling parameters used in this study.

Phonon mode	Energy (meV)	Coupling strength ( $10^{-3}$ eV <sup>2</sup> )
Intravalley LO	195	23.25
Intravalley RBM	28	0.95
Intervalley TA/LO <sup>a</sup>	156	0.19
Intervalley LO/TA <sup>a</sup>	183	44.64

<sup>a</sup>Zone-boundary phonon modes that mediate intervalley scattering are found to be a mixture of fundamental polarizations.

<sup>a)</sup>Electronic mail: dmitri.e.nikonov@intel.com

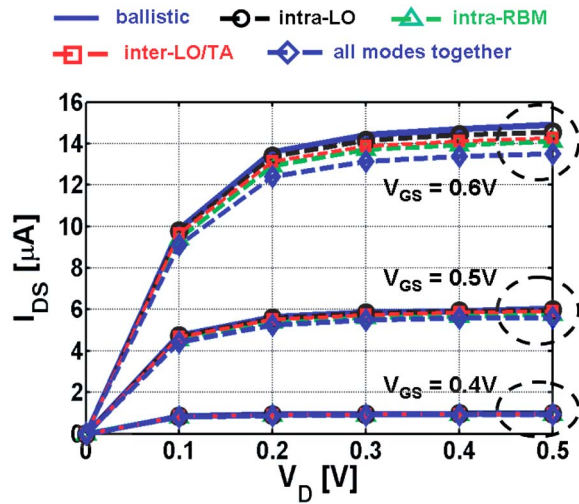


FIG. 1. (Color online)  $I_{DS}$ - $V_{DS}$  under ballistic transport and phonon scattering for  $V_{GS}=0.4, 0.5,$  and  $0.6$  V. Curves are grouped by  $V_{GS}$  for clarity. The inter-TA/LO mode (not shown above) does not affect the ballisticity in the above voltage bias range.

$$R_{e-OP} = \frac{\hbar |M_{OP}|^2 J_1^2}{2nm_C \omega_{OP}}, \quad (1)$$

where  $m_C$  is the mass of a carbon atom, the deformation potential  $J_1=6$  eV/Å,  $\omega_{OP}$  is the frequency of the phonon mode, and the reduced matrix elements  $|M_{OP}|^2$  are calculated according to Ref. 19. The scattering self-energies are determined according to Ref. 15.

For the case of acoustic phonons (with energy close to zero for the considered phonon momenta) the electron-phonon coupling strength is determined by<sup>20</sup>

$$R_{e-AP} = \frac{D_{AP}^2 k_B T}{nm_C v_L^2}, \quad (2)$$

where the deformation potential for acoustic phonons is  $D_{AP}=3J_0$  and the speed of sound  $v_L=21.1$  km/s.<sup>20</sup> The energy dependent scattering rate,  $\tau_{AP}^{-1}(E)$ , is given by

$$\tau_{AP}^{-1}(E) = 2\pi R_{e-AP} \Delta x \text{DOS}(E)/\hbar, \quad (3)$$

where  $\text{DOS}(E)$  is the local density of states per spin state per band valley,<sup>15</sup> and the carbon-carbon bond length is  $a_{CC}=1.42$  Å. Green's functions are normalized per ring of a zigzag nanotube, each containing  $n$  atoms. The average distance between the rings is  $\Delta x=3a_{CC}/4$  and the relation between the density of state and the electron and hole Green's functions is  $\text{DOS}=(G^n+G^p)/2\pi\Delta x$ . Note that the high-energy mean free path for optical or acoustic phonon scattering, related to coupling constant via the hopping parameter  $J_0=3$  eV,<sup>19</sup>

$$\lambda_{hi} = \frac{3a_{CC}J_0^2}{2R_{e-p}} \quad (4)$$

has a clear meaning only for the linear portion of the electronic dispersion curve at large energies or for metallic nanotubes. The effective mean free path depends on the density of states and Fermi filling factors and could be much smaller than  $\lambda_{hi}$  near the band edge of semiconducting CNTs.

We first consider the role of scattering in influencing the  $I_{DS}$ - $V_{DS}$  characteristics for various phonon modes with non-zero energy (Fig. 1). We find that the reduction of drain

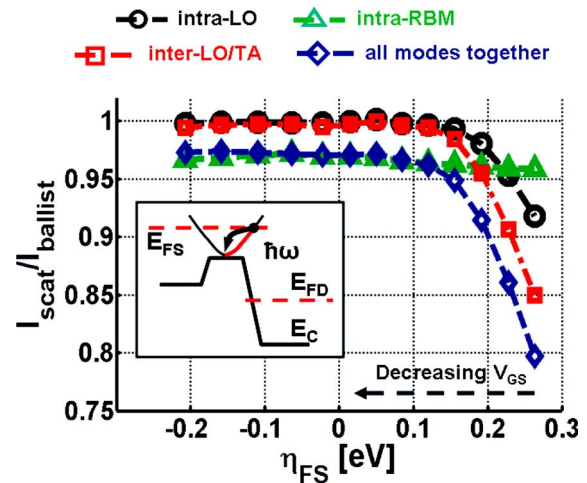


FIG. 2. (Color online) Ballisticity ( $I_{\text{scat}}/I_{\text{ballist}}$ ) vs  $\eta_{FS}$  under phonon scattering at  $V_{DS}=0.4$  V. Here,  $\eta_{FS}$  is the energy difference between the source Fermi level and the channel injection barrier. Negative (positive)  $\eta_{FS}$  corresponds to small (large)  $V_{GS}$  values.  $V_{GS}$  is varied from 0.2 to 0.8 V in steps of 0.05 V. Inset: at large  $V_{GS}$  ballisticity decreases due to OP emission.

current due to scattering increases with gate bias. This bias dependence is better understood by examining the ballisticity (defined as the ratio between current under scattering and the ballistic current,  $I_{\text{scat}}/I_{\text{ballist}}$ ) as shown in Fig. 2. Ballisticity is plotted against  $\eta_{FS}$ , the energy difference between the source Fermi level and the channel injection barrier. (The significance of  $\eta_{FS}$  is explained by the inset of Fig. 2.) Under ballistic operation at a fairly large drain bias, only the positive going states in the channel region are filled by the source Fermi distribution. In order for electrons to backscatter due to phonon emission, two main requirements must be satisfied: (1) the positive going electrons should be higher than the band edge by at least the amount of phonon energy and (2) there should be an empty negative going state that the electron can backscatter into. Note that it is the scattering in the channel that matters most. When electrons reach the drain region they can emit optical phonons and scatter into empty low-energy states. However, if the phonon energy is large, such backscattered electrons would not have enough energy to cross over the channel injection barrier and reach the source region, and the scattering process has a minimal effect on steady-state current transport.<sup>9,21</sup>

Under low  $V_{GS}$ , the conduction band edge in the channel is above  $E_{FS}$ , and  $\eta_{FS}<0$ . The electronic states in the channel with much higher energies than the source Fermi energy ( $E_{FS}$ ) are occupied with an exponentially decaying tail of the Fermi distribution. Thus only a small fraction of the electrons crossing the barrier has enough energy to experience scattering by an optical phonon. This corroborates the results<sup>9</sup> that ballisticity for optical phonons can be close to unity. Note in Fig. 2 that for negative  $\eta_{FS}$ , lower energy phonons, especially with energies comparable to thermal energy,  $k_B T$  (e.g., 28 meV intravalley RBM), cause a larger decrease of current, since they can scatter back to the source, overcoming the channel injection barrier.<sup>21</sup> The importance of RBM scattering in CNTs for carrier transport has recently been reported.<sup>20,22,23</sup> Experimentally, the effect of various phonon modes on current transport can be manifested by comparing suspended and covered nanotube transistors.<sup>24</sup> In the former, all phonon modes are present. In the latter, the out-of-plane phonon modes (RBM) are likely to be effec-

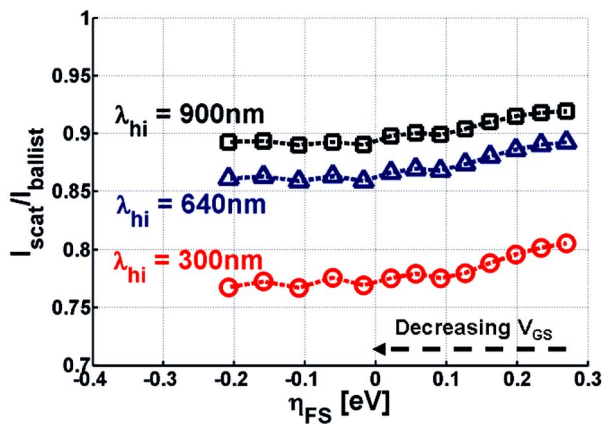


FIG. 3. (Color online) Ballisticities (variables same as in Fig. 2) under acoustic phonon scattering for various high-energy mean free paths [ $\lambda_{hi}$  from Eq. (4)].  $\lambda_{hi}=640$  nm corresponds to the theoretically determined electron-phonon coupling from Eq. (2).

tively clamped. Thus we expect transport to be more ballistic and current to be higher in transistors with covered nanotubes. As discussed in Ref. 23, the presence or absence of the RBM may explain recent experiments.<sup>24</sup>

On the other hand, for higher  $V_{GS}$  when  $\eta_{FS} > 0$ , a significant fraction of electrons crossing the channel injection barrier is backscattered by every phonon mode present. As a result, the ballisticities decrease significantly when  $\eta_{FS} \geq \hbar\omega$ . Examining Fig. 2 confirms that the onset of ballisticities roll off for progressively higher phonon energies occurs at increasingly larger gate biases. As stated in Table I, the higher energy phonons [e.g., intervalley longitudinal optical and transverse acoustic (LO/TA, 183 meV) and intravalley LO (195 meV)] have greater electron-phonon coupling constants. This results in a greater decrease of current (i.e., lower ballisticity) due to scattering via these phonon branches at larger  $V_{GS}$ , once such scattering becomes effective.

Figure 2 also shows the ballisticities when all phonon modes of Table I are simultaneously active (“all modes”). In most of the cases, the decrease of current is a combination of decrease from each mode. The interesting exception is that ballisticities for all modes is higher than for the 28 meV RBM alone at low gate bias. In the case of low-energy phonons, such as the 28 meV RBM, backscattering near the drain region leaves carriers with enough energy to cross the channel barrier and to reach the source region, thereby contributing to reduction of ballisticity. But, in the presence of high-energy phonons, carriers near the drain are scattered again into lower energy states that cannot overcome the channel barrier, thus enhancing the overall ballisticity.

Finally, we discuss ballisticity under acoustic phonon scattering. For elastic scattering, experimentally deduced mean free paths for metallic CNTs are reported to be anywhere from 300 nm to more than 1  $\mu\text{m}$ .<sup>3-5</sup> They could potentially include contributions from other types of elastic scattering mechanisms as well. The high-energy mean free paths ( $\lambda_{hi}$ ) investigated in this study, listed in Fig. 3, are for the lower and upper bounds of experimental data as well as for the theoretical value,  $\lambda_{hi}=640$  nm, from Eqs. (2) and (4) for the case of (13,0) CNT. It is interesting that the overall change in ballisticity with elastic scattering (Fig. 3) is very different from that in the inelastic scattering case (Fig. 2).

The ballisticity with only acoustic (elastic) phonon scattering increases by about 5% with gate bias while inelastic scattering causes the ballisticity to decrease with gate bias. The reason for this is that at low  $V_{GS}$  (off state) the current is primarily determined by carriers at the conduction band edge of the channel injection barrier. Due to the large density of states near the conduction band edge in one-dimensional (1D) systems (Van Hove singularity), such carriers experience a higher scattering rate as indicated by Eq. (3). Therefore, they have a smaller effective mean free path compared with the channel length, resulting in a reduction in the ballisticity. At large  $V_{GS}$ , however, a significant fraction of carriers occupy states well above the conduction band edge where the scattering rate is much lower, resulting in an increase in ballisticity. It is quite surprising that the ballisticity is as small as 0.77 when the high-energy mean free path [ $\lambda_{hi}$  from Eq. (4)] is about 15 times larger than the channel length. Nevertheless, such reduction of the current can be attributed to 1D nature of transport where each elastic scattering event amounts to backscattering of the carriers.<sup>9,21</sup>

The authors acknowledge the support of this work by the NASA Institute for Nanoelectronics and Computing (NASA INAC NCC 2-1363), NASA contract NAS2-03144 to UARC, and Intel Corporation. Computational support was provided by the NSF Network for Computational Nanotechnology (NCN).

- <sup>1</sup>S. Frank, P. Poncharal, Z. L. Wang, and W. A. de Heer, *Science* **280**, 1744 (1998).
- <sup>2</sup>J. Kong, E. Yenilmez, T. W. Tombler, W. Kim, and H. Dai, *Phys. Rev. Lett.* **87**, 106801 (2001).
- <sup>3</sup>Z. Yao, C. L. Kane, and C. Dekker, *Phys. Rev. Lett.* **84**, 2941 (2000).
- <sup>4</sup>J.-Y. Park, S. Rosenblatt, Y. Yaish, V. Sazonova, H. Üstünel, S. Braig, T. A. Arias, P. W. Brouwer, and P. L. McEuen, *Nano Lett.* **4**, 517 (2004).
- <sup>5</sup>A. Javey, J. Guo, M. Paulsson, Q. Wang, D. Mann, M. Lundstrom, and H. Dai, *Phys. Rev. Lett.* **92**, 106804 (2004).
- <sup>6</sup>A. Svizhenko and M. P. Anantram, *Phys. Rev. B* **72**, 085430 (2005).
- <sup>7</sup>A. Javey, J. Guo, Q. Wang, M. Lundstrom, and H. Dai, *Nature (London)* **424**, 654 (2003).
- <sup>8</sup>Ph. Avouris, R. Martel, V. Derycke, and J. Appenzeller, *Physica B* **323**, 6 (2002).
- <sup>9</sup>J. Guo and M. Lundstrom, *Appl. Phys. Lett.* **86**, 193103 (2005).
- <sup>10</sup>J. Guo, *J. Appl. Phys.* **98**, 063519 (2005).
- <sup>11</sup>F. Leonard and J. Tersoff, *Phys. Rev. Lett.* **88**, 258302 (2002).
- <sup>12</sup>J. Guo, A. Javey, H. Dai, and M. Lundstrom, *Tech. Dig. - Int. Electron Devices Meet.* **2004**, 703.
- <sup>13</sup>G. Pennington and N. Goldsman, *Phys. Rev. B* **68**, 045426 (2003).
- <sup>14</sup>A. Verma, M. Z. Kauser, and P. P. Ruden, *J. Appl. Phys.* **97**, 114319 (2005).
- <sup>15</sup>S. Datta, *Quantum Transport: Atom to Transistor*, 2nd ed. (Cambridge University Press, Cambridge, UK, 2005), Chap. 10.
- <sup>16</sup>A. Svizhenko, M. P. Anantram, T. R. Govindan, B. Biegel, and R. Venugopal, *J. Appl. Phys.* **91**, 2343 (2002).
- <sup>17</sup>J. Guo, S. Datta, M. Lundstrom, and M. P. Anantram, *Int. J. Multiscale Comp. Eng.* **2**, 60 (2004); e-print cond-mat/0312551.
- <sup>18</sup>R. Saito, G. Dresselhaus, and M. S. Dresselhaus, *Physical Properties of Carbon Nanotubes* (Imperial College Press, London, 1998).
- <sup>19</sup>G. D. Mahan, *Phys. Rev. B* **68**, 125409 (2003).
- <sup>20</sup>G. Pennington and N. Goldsman, *Phys. Rev. B* **71**, 205318 (2005).
- <sup>21</sup>M. Lundstrom, *IEEE Electron Device Lett.* **18**, 361 (1997).
- <sup>22</sup>V. Perebeinos, J. Tersoff, and Ph. Avouris, *Phys. Rev. Lett.* **94**, 086802 (2005).
- <sup>23</sup>A. Verma, M. Z. Kauser, and P. P. Ruden, *Appl. Phys. Lett.* **87**, 123101 (2005).
- <sup>24</sup>E. Pop, D. Mann, J. Cao, Q. Wang, K. Goodson, and H. Dai, *Phys. Rev. Lett.* **95**, 155505 (2005).

## Ballistic of nanotube field-effect transistors: Role of phonon energy and gate bias

Siyuranga O. Koswatta, Sayed Hasan, Mark S. Lundstrom, M. P. Anantram, and Dmitri E. Nikonov

Citation: [Applied Physics Letters](#) **89**, 023125 (2006); doi: 10.1063/1.2218322

View online: <http://dx.doi.org/10.1063/1.2218322>

View Table of Contents: <http://scitation.aip.org/content/aip/journal/apl/89/2?ver=pdfcov>

Published by the [AIP Publishing](#)

---

### Articles you may be interested in

[Tunable ambipolar Coulomb blockade characteristics in carbon nanotubes-gated carbon nanotube field-effect transistors](#)

Appl. Phys. Lett. **94**, 022101 (2009); 10.1063/1.3065067

[Local silicon-gate carbon nanotube field effect transistors using silicon-on-insulator technology](#)

Appl. Phys. Lett. **89**, 023116 (2006); 10.1063/1.2221515

[Air-stable n -type carbon nanotube field-effect transistors with Si<sub>3</sub>N<sub>4</sub> passivation films fabricated by catalytic chemical vapor deposition](#)

Appl. Phys. Lett. **86**, 113115 (2005); 10.1063/1.1886898

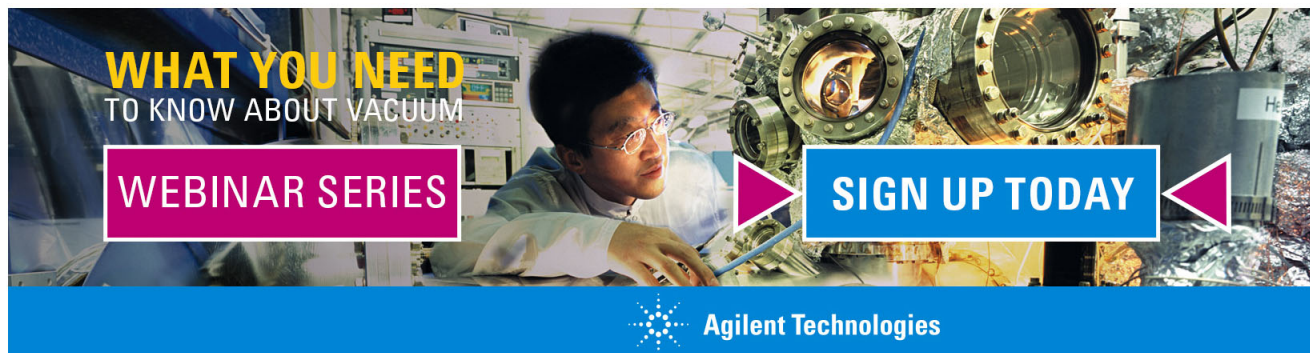
[Characteristics of a carbon nanotube field-effect transistor analyzed as a ballistic nanowire field-effect transistor](#)

J. Appl. Phys. **97**, 034306 (2005); 10.1063/1.1840096

[Silicon nitride gate dielectric for top-gated carbon nanotube field effect transistors](#)

J. Vac. Sci. Technol. B **22**, 3112 (2004); 10.1116/1.1824048

---

A promotional banner for a webinar series. The background is a photograph of a man in a white lab coat and glasses working in a laboratory with various pieces of equipment. Overlaid on the image are several text elements: 'WHAT YOU NEED TO KNOW ABOUT VACUUM' in yellow and white text at the top left; 'WEBINAR SERIES' in white text on a pink rectangular background at the bottom left; 'SIGN UP TODAY' in white text on a blue rectangular background at the bottom right, flanked by two pink triangles pointing towards each other; and the Agilent Technologies logo and name in white on a blue background at the bottom center.